Neuron, Vol. 20, 1283–1294, June, 1998, Copyright ©1998 by Cell Press

Three Transmembrane Conformations and Sequence-Dependent Displacement of the S4 Domain in Shaker K^+ Channel Gating

O. S. Baker,*§ H. P. Larsson,†§‖ L. M. Mannuzzu,† and E. Y. Isacoff†*‡
*Group in Biophysics
†Department of Molecular and Cell Biology
University of California, Berkeley
Berkeley, California 94720-3200

Summary

We have acquired structural evidence that two components evident previously in the depolarization-evoked gating currents from voltage-gated Shaker K^+ channels have their origin in sequential, two-step outward movements of the S4 protein segments. A point mutation greatly destabilizes the "fully retracted" state of S4 transmembrane translocation, causing instead an intermediate state to predominate at resting potentials. This state is distinguishable topologically and fluorometrically. That a point mutation effectively excludes half the range of S4 motion from physiological voltages suggests that the diverse sensitivities among voltage-gated channels might reflect not only differences in S4 valence, but also displacement. Existence of an intermediate subunit state helps explain why modeling channel activation has required positing greater than four closed states.

Introduction

Hodgkin and Huxley (1952) hypothesized that voltage controls the conductance of membranes by biasing the equilibrium of charged gating particles between two stable positions within the transmembrane electric field. The S4 motif of basic residues, which is conserved within the primary structure of voltage-gated ion channels, has been hypothesized to confer voltage sensitivity by such a mechanism (Greenblatt et al., 1985; Noda et al., 1984; Guy and Seetharamulu, 1986). In support of this hypothesis, distinct transmembrane-topological states of S4 have been shown to be associated with the resting and the open conformations of both Shaker K^+ channels (Larsson et al., 1996; Mannuzzu et al., 1996; Yusaf et al., 1996) and hSkMI Na^+ channels (Yang and Horn, 1995; Yang et al., 1996, 1997). These studies indicate that membrane depolarization moves S4 outwards, consistent with its positive charge, the polarity of gating currents, and the gating-particle hypothesis. The extent of this motion appears sufficient to account for the total gating charge. Furthermore, decrements in gating charge caused by charge-neutralizing S4 substitutions in Shaker channels are consistent with the hypothesis that the S4 charges make up most or all of the charge total (Aggarwal and MacKinnon, 1996; Seoh et al., 1996).

On the other hand, numerous studies have shown that Shaker channel activation, in detail, cannot be explained in terms of a single, two-state gating particle domain in each channel subunit (Schoppa et al., 1992; Bezanilla et al., 1994; McCormack et al., 1994; Sigg et al., 1994; Sigworth, 1994; Stefani et al., 1994; Zagotta et al., 1994b). In particular, gating current recordings from Shaker channels, as well as from chimeric channels possessing the transmembrane core of the mammalian Shaker homolog, Kv1.1, exhibit two components, which Bezanilla and coworkers have termed Q_1 and Q_2 (Stuhmer et al., 1991; Bezanilla et al., 1994; Stefani et al., 1994). The existence of two components suggests that either, besides S4, there exists another "auxiliary" gating particle domain; or that S4 displacement occurs not in a single step, but instead in two steps, via an intermediate state. Independently, recent evidence from mutagenesis and voltage-clamp fluorescence suggests that an auxiliary gating particle domain might be comprised by an acidic residue in S2 (Seoh et al., 1996; Cha and Bezanilla, 1997).

We wished to examine whether the two distinguishable phases of gating-charge movement, Q_1 and Q_2, which characterize the activation of Shaker channels by voltage, actually involve two distinct steps in the transmembrane (tm) translocation of one gating-particle domain, S4. We applied the technique of voltage-clamp fluorometry, or VCF (Mannuzzu et al., 1996), involving the covalent coupling of a reporter fluor to an S4-substituted cysteine, to investigate whether changes in the microenvironment around S4 correlate with Q_1 and Q_2. And to examine whether such changes arise from changes in S4 tm topology, we assayed the voltage-dependent accessibility of S4-substituted cysteines from both sides of the membrane using the impermeant, thio-reactive reagent, methanethiosulfonate ethyltrimethyl ammonium (MTSET; Akabas et al., 1992; Stauffer and Karlin, 1994). To be able to resolve structural changes associated with Q_1 from those associated with Q_2, we took advantage of the properties of mutant channels possessing the substitution, R365C or R365S, within S4. These channels exhibit a voltage dependence of gating-charge movement which, like the wild type (wt), is described by two components, but whose components, unlike the wt, activate over almost entirely nonoverlapping voltage ranges. Thus, simply by voltage clamping, we have been able to "isolate" and to probe biochemically a gating-charge intermediate.

We find that the S4 domain of Shaker K^+ channel subunits transits between three conformational states during the activation of channels by voltage: (i) a state in which S4 is maximally retracted into the cell, which characterizes resting subunits, (ii) a state in which S4 is displaced maximally outward, which characterizes fully activated subunits, and (iii) a state of intermediate S4 displacement, which characterizes a stable intermediate in the movement of gating charge and the activation of channel subunits. Displacement of S4 from the resting to the intermediate position correlates with Q_1, and that from the intermediate to the fully activated position correlates with Q_2.

‡To whom correspondence should be addressed.
§These two authors contributed equally to this work.
‖Present address: Nobel Institute for Neurophysiology, Department of Neuroscience, Karolinska Institutet, S-171 77 Stockholm, Sweden.

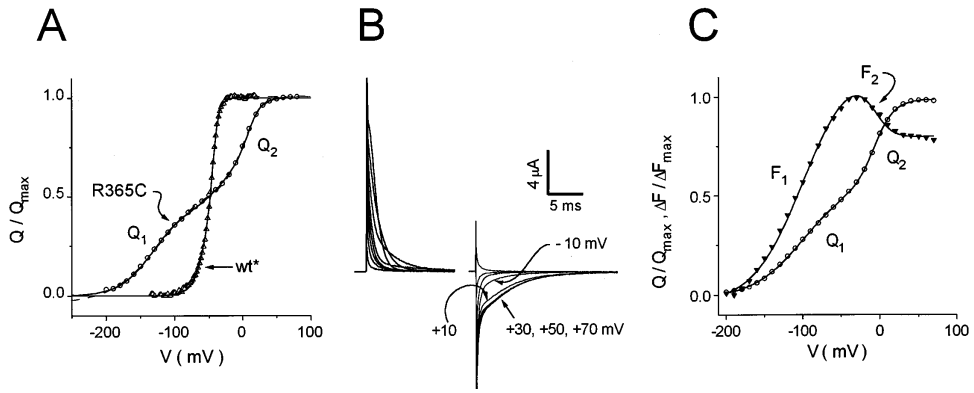

Figure 1. "Two-Step" Gating in R365C and R365S Channels

(A) Shaker channels that posses the R365C substitution in S4 exhibit two resolved components ("Q_1" and "Q_2") in their gating-charge voltage-dependence (Q-V). In the wild-type Q-V (wt*, data from Bezanilla et al., 1994) two components exist but overlap. Superimposed fits are to the model of Figure 7 (solid lines) and to the sum of two "Boltzmanns" (dashes): $Q = \{Q_1 (1 + \exp[-Z_1 F(V - V_1)/RT])^{-1} + Q_2(1 + \exp[-Z_2 F(V - V_2)/RT])^{-1}\}$, where R, F, and T have their conventional meanings. Boltzmann parameters (Q_1, Z_1, V_1; Q_2, Z_2, V_2) were all fit freely. For R365C they are (0.59, 0.73, −123 mV; 0.45, 1.86, 1 mV) for the Q-V shown and (0.60 ± 0.02, 0.63 ± 0.07, −133 ± 11 mV; 0.40 ± 0.02, 2.24 ± 0.40, 1 ± 4 mV) are the means ± SE for 10 oocytes. For the wt Q-V data from Bezanilla and coworkers (1994) they are (0.27, 2.3, −65 mV; 0.73, 4.86, −46 mV). Fitted model parameters (V_1, V_2, V_c) are (−134 mV, −18 mV, −1 mV) for the R365C Q-V shown and (−44 mV, −51 mV, −80 mV) for the wt Q-V of Bezanilla and coworkers. Fixed parameters (z_1, z_2, z_c) are (1.07, 0.99, 1.8) and (1.93, 1.06, 1.8) for R365C and wt, respectively, and are described in the Figure 7 legend (note that z_1, z_2 are per-subunit values, while z_c is for the channel as a whole). Note that the Boltzmann fit predicts a larger Q_1 for R365C than does the model fit (discussed in Experimental Procedures). R365C charge was measured from steps to +40 mV following prepulses of 25–30 ms duration to the indicated potentials.

(B) R365C "On" and "Off" gating currents evoked by steps from −80 mV hp to voltages ranging −70–+70 in 20 mV increments, followed by repolarization to −60 mV. At the −80 mV hp, about 75% of Q_1 is already activated (see [A]). The small fast On seen for small depolarizations represents the remaining 25%. The slowing of the On and the Off in response to the larger depolarizations parallels that in wild-type activation gating. The On, Off, and the holding current have been separately baseline adjusted for display.

(C) (Open circles) Representative Q-V for S352C-TMRM/R365S channels, exhibiting two well-resolved components ("Q_1" and "Q_2"). Superimposed curve is a free two-Boltzmann fit (0.58, 0.78, −100 mV; 0.42, 1.99, −7 mV). (Filled triangles) F-V for the same channels acquired by VCF also exhibits two components ("F_1" and "F_2"). Superimposed curve is the sum of two Boltzmanns with all voltage-dependent parameters taken from the Q-V fit, and only the amplitudes ($F_1 = 1.23$, $F_2 = -0.37$) adjusted to fit the size and polarity of the fluorescence changes. The level of agreement of Q_1 with F_1 and Q_2 with F_2 implied by the fit is representative: Chi-squared for the constrained fit applying the Q-V parameters to the F-V curve is $\chi^2 = 0.00015$ for the oocyte shown, and $<\chi^2> = 0.00024 \pm 0.00015$ for the mean of seven equivalent data sets.

These results have implications both for the mechanism by which voltage controls the conductivity of Shaker channels, and for a possible mechanistic basis for the diversity of voltage sensitivities exhibited by channels of like S4 valence.

Results

R365C Enables Study of a Gating-Charge Intermediate in the Steady State

In Shaker channels with wild-type activation gating (see Experimental Procedures regarding channel nomenclature), the voltage dependencies of Q_1 and Q_2 overlap closely (Bezanilla et al., 1994; Stefani et al., 1994; and see also Figure 1A). Therefore, it is not possible to isolate them *en masse* in a state in which Q_1 has moved but Q_2 has not. However, the charge–voltage relations (Q-Vs) of Shaker channels in which the second basic residue of S4, R365, has been neutralized by substitution with either cysteine (Figure 1A), serine (Figure 1C), or glutamine (Aggarwal and MacKinnon, 1996; Seoh et al., 1996) exhibit two components that do not overlap. These components share features of Q_1 and Q_2 in wild-type activating channels. First, the two components both comprise a large fraction of the total gating charge. Second, their relative amplitudes are incommensurate to their relative slopes; such that in both R365C (Figure 1A) and in wild-type activating channels (Bezanilla et al., 1994; Stefani et al., 1994) the more depolarized component is disproportionately steep—suggesting positive cooperativity between channel subunits in the conformational transitions between states nearer to the open state (Bezanilla et al., 1991; Schoppa et al., 1992; Tytgat and Hess, 1992; Zagotta et al., 1994a, 1994b; Schoppa and Sigworth, 1998; L. M. M. and E. Y. I., unpublished data; O. S. B. and E. Y. I., unpublished data). Finally, the "On" and "Off" gating currents (I_g) that are evoked by step depolarizations large enough to move both charge components are slower than those that move only the more hyperpolarized-activating one (Figure 1B).

In analogy to wild-type activating channels, we will refer to the more hyperpolarized and more depolarized components of R365C charge movement as Q_1 and Q_2. Furthermore, the features common between Q_1 and Q_2 in R365C and in wild-type activating channels, and the fact that the two channels differ by only a single amino acid, strongly suggest that the mechanism of charge displacement is conserved between the two. Therefore, we proposed to use Q_1 and Q_2 movement in R365C channels as a means to gain insights into the conformational changes that give rise to Q_1 and Q_2 in wild-type activating Shaker channels.

Fluorescence Suggests Q_1 and Q_2 Are Distinct S4 Movements

We applied VCF to channels in which R365 was neutralized. As a fluorescent reporter of conformational movements in the vicinity of S4, we used tetramethylrhodamine maleimide (TMRM) attached to the substituted cysteine, 352C, in the S3/S4 loop. In channels in which residue 365 is the native arginine, 352C-TMRM gives rise to a large ΔF that correlates closely with the wt-like charge movement that these channels exhibit (L. M. M. and E. Y. I., unpublished data). We wanted to examine the effect that neutralizing R365 would have on the voltage dependence of fluorescence (F-V) reported by 352C-TMRM. In order to fluorescently tag only 352C, we neutralized R365 in this instance with serine. S352C-TMRM/R365S channels exhibited a biphasic Q-V relation similar to R365C channels, and exhibited a biphasic F-V relation (Figure 1C), in which the two components correlate closely with their charge counterparts (both with regard to slope and midpoint). Notably, the S4-associated conformational changes correlating with Q_1 and Q_2 give rise to opposing changes in the brightness of the 352C-coupled fluor (Figure 1C), implying that they are qualitatively different.

To determine whether these changes reflect sequential tm translocations of S4, such as would be capable of generating the large gating charge fractions observed, we undertook to characterize them topologically.

A "Double-Reporter" Channel for Assaying TM Topological Changes

Topological characterization required a means to assay for changes at both the external and cytosolic boundaries of the transmembranous region of S4. We have shown previously that 365C itself is a reporter of movement at the external tm boundary of S4, and that it does not enter the cytosol at voltages sufficient to deactivate wild-type activating channels (Larsson et al., 1996). Subsequently, the observation of an extremely negative component of the Q-V (i.e., Q_1), and the large absolute decrement in charge caused by the R365Q substitution (Aggarwal and MacKinnon, 1996; Seoh et al., 1996), prompted us to examine whether 365C becomes cytosolically accessible at extremely negative voltages. We observed no modification of R365C channel gating during 5–10 mM s cumulative exposure to internal MTSET at −150 to −200 mV in excised patches from 6 oocytes (data not shown). Thus, the cytosolic accessibility of 365C even in fully deactivated channels (i.e., channels in which neither Q_1 nor Q_2 has been activated) is exceptionally low (discussed further below). Furthermore, internal perfusion of more than 5–10 mM s MTSET consistently destroyed inside-out patches clamped even only intermittently to the voltages necessary to deactivate Q_1. Therefore, cysteine at 365 could not be used as a reporter of voltage-dependent changes at the internal tm boundary of S4 as it could for the external boundary.

Consequently, we decided to construct a channel containing two S4 cysteine substitutions, or a "double-reporter" channel. To R365C we added the additional cysteine substitution F370C. Based on the pattern of accessibilities observed in our previous study (Larsson et al., 1996), we predicted that cysteine at position 370 would be accessible to internally perfused MTSET in the resting state and be inaccessible in the open state. In perfused inside-out patches we observed no MTSET modification of conducting F370C channels that were held open at a voltage of +100 mV (Figure 2B, open symbols; 14–20 mM s MTSET, n = 4). However, modification did occur when channels were perfused with MTSET while held closed at −100 mV (Figure 2B, filled symbols), and the rate of modification, k, was not significantly accelerated by further hyperpolarization [k(−100 mV) = 0.15 ± 0.01 mM^{-1} s^{-1}, n = 4; k(−150 mV) = 0.16 ± 0.03 mM^{-1} s^{-1}, n = 4; calculated as described in Experimental Procedures]. Conveniently, the effect of MTSET modification was distinguishable in nature from its effect on R365C channels (Larsson et al., 1996), causing an elimination of evocable currents over the clampable voltage range (Figure 2A). Furthermore, the pairing of the F370C substitution with R365C resulted in channels that exhibited a Q-V relation (Figure 4C)

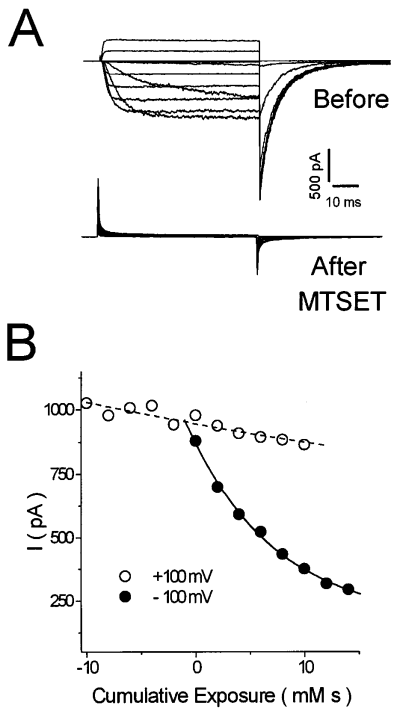

Figure 2. State-Dependent Internal MTSET Modification of F370C Channels

(A) F370C channel currents from an excised patch in symmetrical potassium solutions. hp = −100 mV. V_{tail} = −65 mV. V_{test} = −80–+20 mV, steps in 10 mV increments before and after perfusion of the cytosolic patch face with 60 mM s MTSET.

(B) Modification time courses for two perfusion protocols superimposed. Steady-state amplitude of currents evoked by periodic 25 ms test pulses to +100 mV during perfusion of 4 mM MTSET for 500 ms every 10 s, on channels clamped initially open ("+100 mV") and then closed ("−100 mV;" as in Figure 3 of Larsson et al., 1996). Abscissa, [application time] × [concentration MTSET]. 0 marks onset of MTSET perfusion. Only in closed channels ("−100 mV") did MTSET perfusion cause a diminution of currents above the basal rate of rundown ("+100 mV"), implying inaccessibility of 370C in activated channel subunits.

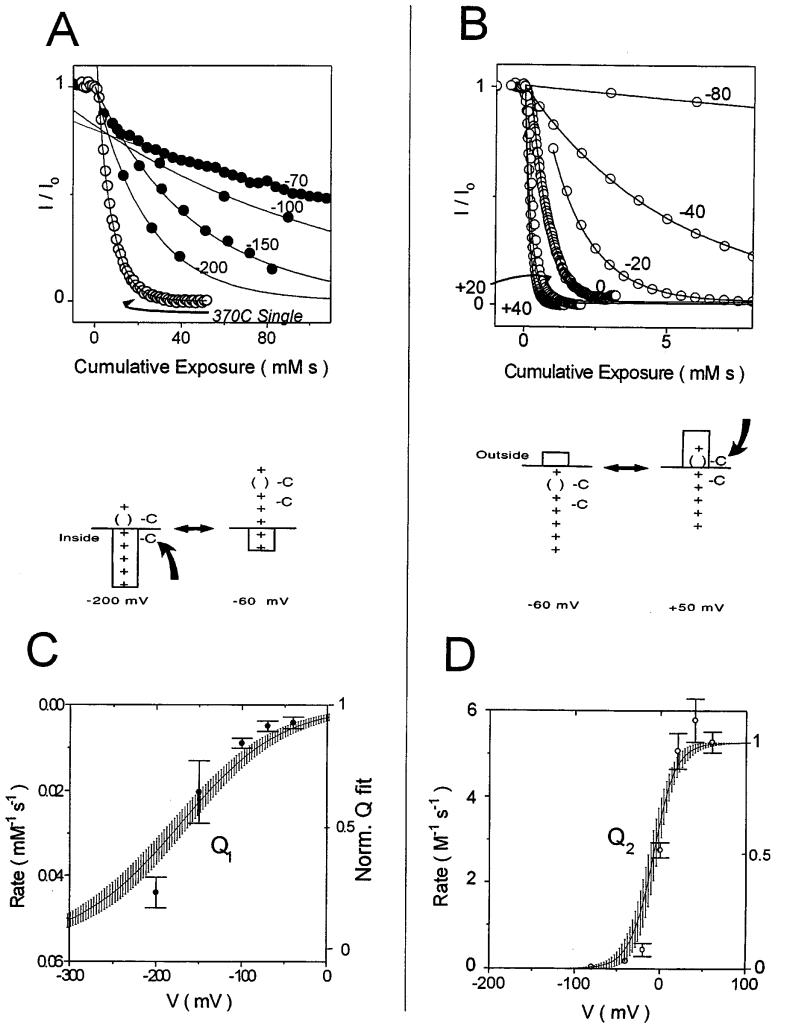

Figure 3. Voltage Dependencies of Internal and External MTSET Modification of R365C/F370C Channels Do Not Coincide

(A) Time courses of internal modification. Points chart the steady-state amplitude of currents evoked by periodic 25 ms test pulses to +100 mV, with perfusion of MTSET confined to steps to the indicated potentials for 365C/370C channels (filled circles), and to −100 mV for 370C channels (open circles). Abscissa, [application time] × [concentration MTSET]. Note that hyperpolarization speeds internal modification. Cartoon interprets this observation in terms of the internal S4 tm boundary.

(B) Time courses of external MTSET modification. Steady-state currents in response to 25 ms test pulses to +80 mV (see Experimental Procedures), in continuously perfused whole oocytes clamped to the indicated potentials 50% of the time. Abscissa, [application time] × [concentration MTSET]. Note that depolarization speeds external modification. Cartoon interprets this observation in terms of the external S4 boundary.

(C) Voltage dependence of the calculated rate of internal modification at the indicated voltages. Rate is calculated as the reciprocal of the time constant of the monoexponential fit of the time course of modification as plotted in (A) and (B). Q_1 curve is the first component from two-Boltzmann fits to R365C/F370C channel Q-Vs (mean of 4); and has been scaled (but not offset) for comparison with the rates. Error bars = ± SD for both the curve and the rate data.

(D) Voltage dependence of the calculated rate of external modification at the indicated voltages. Q_2 was derived and scaled as described for Q_1 in (C).

qualitatively unaltered with respect to that seen in channels possessing the R365C substitution alone (Figures 1A and 4B). Therefore, we concluded that the double-reporter channels could be used to relate Q_1 and Q_2 to changes in S4 tm topology.

Distinguishing Three TM Topological States of S4

Our strategy was to characterize in R365C/F370C channels the voltage dependencies with which channels would gain or lose their independent susceptibilities to modification by internal and by external MTSET. If Q_1 and Q_2 arise from translocation of S4 in two sequential steps, we would expect that the two voltage dependencies might not coincide: partial movement of S4 during Q_1 being sufficient to render 370C inaccessible to the cytosol, for example, but insufficient to project 365C into the extracellular solution.

We assayed internal modifiability in excised inside-out patches and external modifiability in externally perfused, whole oocytes under two-electrode voltage clamp (see Larsson et al., 1996, and Experimental Procedures). As was observed in channels into which cysteine was substituted at position 370 alone, modification by internal MTSET of the double-reporter channels resulted in the elimination of ionic currents (data not shown). Compared to the time course observed for F370C channels at −100 mV (Figure 3A, open symbols), modification of R365C/F370C channels at the same voltage proceeded slowly (Figure 3A, "−100" mV time course). But whereas further hyperpolarization produced no increase in the modification rate of F370C channels (described above), in the double-reporter channels it caused modification to proceed more rapidly; so that modification was, in fact, observable at rates approaching that seen in deactivated F370C channels (Figure 3A). Thus, modification by internal MTSET of the double-reporter channels exhibits the qualitative effect and the deactivation state–dependence of MTSET modification of F370C channels. The cartoon of Figure 3A interprets this result.

Figure 3C shows that the rate of modification by internal MTSET varies with voltage over the same range in which the R365C/F370C channel Q_1 activates, and that its voltage dependence exhibits comparable steepness. Therefore, activation of Q_1 appears closely associated with the displacement of 370C from an internally accessible to an internally inaccessible position.

External MTSET modification of the double-reporter

channels, similar to the modification of those with the R365C substitution alone (Larsson et al., 1996), slowed activation gating and shifted the voltage dependence of opening from a greatly depolarized position back to the approximately wild-type range of voltages (data not shown). At voltages less depolarized than those necessary to significantly activate Q_2, external MTSET modified the double-reporter channels only extremely slowly (Figure 3B "−80" time course). At more depolarized potentials, however, the rate of modification increased and saturated with greater depolarization (Figure 3B, −40 to +40). Thus, modification by external MTSET of R365C/F370C channels exhibits the qualitative effects and the open state–dependence of MTSET modification of R365C channels. The cartoon of Figure 3B interprets this result.

Figure 3D shows that the rate of modification by external MTSET varies with voltage over the same range in which the R365C/F370C channel Q_2 activates, and that its voltage dependence exhibits comparable steepness. Therefore, activation of Q_2 appears closely associated with the displacement of 365C from an externally inaccessible to an externally accessible position.

Together these results show that Q_1 activation results in a change in S4 topology that renders 370C inaccessible, but that 365C does not become exposed to the extracellular solution until a second change in S4 topology occurs with activation of Q_2. Therefore, the tm topology of S4 in R365C/F370C channel subunits in between activation of Q_1 and Q_2—in which both positions 365 and 370 are simultaneously inaccessible—is unlike the two states of S4 topology characterized previously (Larsson et al., 1996) in open and closed channels.

Note that if Q_1 and Q_2 indeed reflect sequential rather than independent gating events, as the above results imply, then the fitting of the Q-V to a two-Boltzmann sum is not strictly appropriate. We find that such a fit leads one to attribute an effective valence to the Q_1 displacement that is smaller than that which is necessary to mathematically describe the Q-V by a more realistic scheme (see Figure 1A and the final section of Results). This may account for the observation that the voltage dependence of the rate of internal modification of 370C is somewhat steeper than that of the mean Q_1 derived analytically from two-Boltzmann fits (Figure 3C).

370C Accessibility at Intermediate Voltages Is Restored by 365C Charge "Reconstitution"

The above results argue that neutralization of the second basic S4 residue, R365, which divides charge movement in Shaker channels into two phases with nonoverlapping voltage dependencies (Figure 1A; Aggarwal and MacKinnon, 1996; Seoh et al., 1996), does so by causing an intermediate state of S4 displacement to predominate at the moderately hyperpolarized potentials, at which S4 would normally be in a maximally "internalized" or "retracted" state. We devised a simple test of this interpretation, which predicts that the restoration of a basic residue to position 365 in R365-neutralized channels ought to restore both the wild-type Q-V and the predominance of a fully retracted state of S4 at moderately hyperpolarized potentials. We again made use of the double-reporter channel, using 370C as a reporter of S4 retraction and using externally applied methanthiosulfonate-ethylammonium, MTSEA (Akabas et al., 1992), to convert 365C to a charged, lysine-like residue.

We recorded gating currents in oocytes from both R365C and the double-reporter channels before and after brief external perfusion of MTSEA (Figure 4A). (Channels were made nonconducting with the W434F substitution [Perozo et al., 1993].) Both channels exhibited a biphasic Q-V prior to MTSEA perfusion (Figures 4B and 4C, open circles). Perfusion of 25 μM MTSEA caused an increase and a slowing of the "On" I_g that was evoked by steps to 0 mV from −80 mV holding potential (hp), which saturated in approximately 30 s (data not shown). Subsequent to washout of MTSEA, channels exhibited a sigmoid Q-V relation, exhibiting two components with voltage dependencies that overlapped in the same approximate voltage range as for channels possessing arginine at position 365 (Figure 1A "wt"; Figures 4B and 4C plus-filled circles). Therefore, in contrast to unmodified R365C and double-reporter channels, R365C-SEA and R365C-SEA/F370C channels do not require extreme hyperpolarization to deactivate, and Q_1 and Q_2 appear to have been "reconstituted."

As the second aspect of the test, we examined how MTSEA modification of 365C affected the accessibility of 370C at moderately hyperpolarized potentials. We pretreated oocytes expressing conducting R365C/F370C channels with a cumulative exposure to external MTSEA that was sufficient to cause complete "charge reconstitution" in nonconducting R365C/F370C channels (2 mM s). We then assayed 370C accessibility in inside-out patches excised from the same oocytes. The currents in these patches exhibited the characteristic kinetics and voltage dependence of those seen in whole oocytes following modification by externally applied MTSEA of both R365C and R365C/F370C channels (data not shown; MTSEA's effect on R365C channels is similar to that of MTSET shown in Larsson et al., 1996). Furthermore, preexposure to external MTSEA did not occlude the modifiability of channels by internal MTSET (Figure 4D). This confirms that the two reporter cysteines are accessible independently and only from opposite sides of the membrane (for the cumulative exposures used). Figure 4D shows that, in contrast to channels that had not been preexposed to external MTSEA [k(*365C/370C*, −100 mV) = 0.0089 ± 0.009 $mM^{-1}\,s^{-1}$, n = 4] modification by internal MTSET at −100 mV of externally premodified double-reporter channels proceeded as rapidly [k(*365C-SEA/370C*, −100 mV) = 0.19 ± 0.08 $mM^{-1}\,s^{-1}$, n = 4] as in F370C, single-cysteine channels [k(*370C*, −100 mV) = 0.15 ± 0.01 $mM^{-1}\,s^{-1}$, as described above]. Thus, "reconversion" of 365C to a positively charged residue restores stability at −100 mV to the S4 topological state in which 370C is internally accessible.

Refined Boundaries of S4 Exposure in the Fully Activated and Deactivated States

The large effect on charge movement caused by R365 neutralization, as well as the report of observations contrasting with our own (Yusaf et al., 1996), prompted us to reexamine the accessibility of S4 positions using more

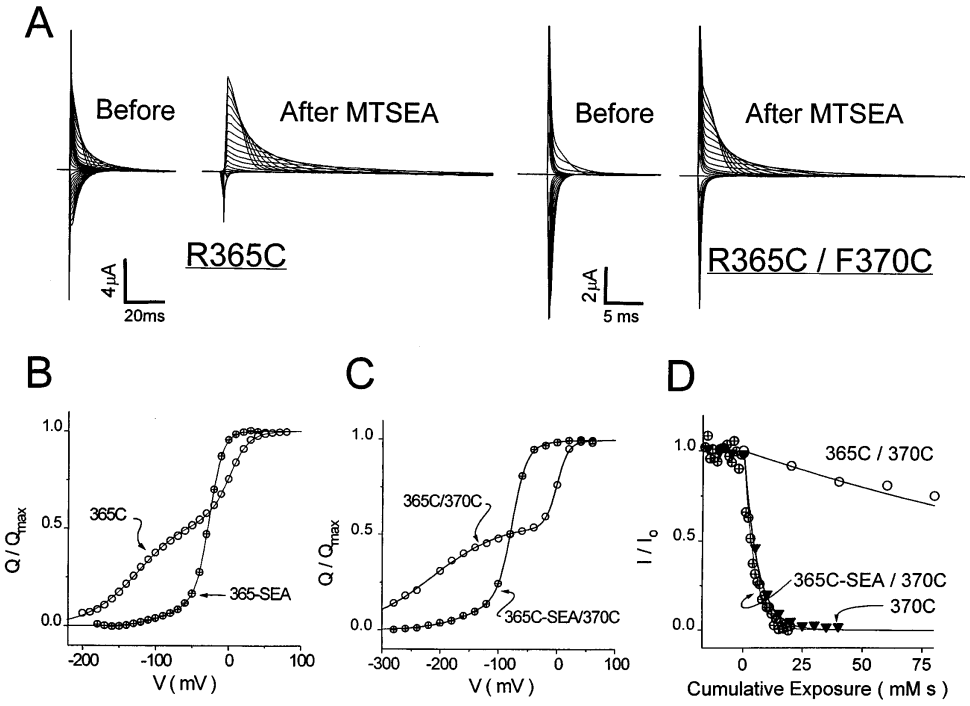

Figure 4. "Reconstitution" of Charge and Accessibility in R365C and R365C/F370C Channels

(A) Representative On gating currents before and after external perfusion and washout of MTSEA, which converts cysteine to a lysine-like residue. R365C and R365C/F370C channels gate similarly and are modified similarly. On and holding current have been separately baseline adjusted for display.

(B) R365C Q-V before ("365C") and after external perfusion of MTSEA ("365C-SEA"). MTSEA makes the Q-V similar to wt (Figure 1A), "reconstituting" Q_1 and Q_2. Q is the integrated I_g at V_{tail} following the prepulse I_g shown in (A). V_{tail} was +40 mV for 365C and −80 mV for 365C-SEA.

(C) R365C/F370C channel Q-V before ("R365C/F370C") and after MTSEA superfusion ("365C-SEA/370C"). The R365C/F370C Q-V resembles that of R365C channels, but Q_1 activation occurs at still more negative voltages. MTSEA reconstitutes Q_1 and Q_2 as in R365C channels in (A). Q was measured as in (B), with V_{tail} = +40 mV for both 365C and 365C-SEA/F370C, excluding the initial 0.5 ms of the transient from the integration of the 365C-SEA/F370C currents.

(D) "Reconstitution" of 370C accessibility. Representative time courses of internal MTSET modification at −100 mV for "double-reporter" channels that were not preexposed to external MTSEA ("R365C/F370C") or were preexposed to 2 mM s external MTSEA ("R365C-SEA/F370C"), and F370C single-cysteine channels (protocol in Figure 3A legend and Experimental Procedures).

extreme voltages and higher cumulative exposures to MTSET.

Previously we deduced the resting-state external boundary of S4 to lie between R365 and R362. We had observed that 356C, 359C, 362C, and 365C exhibited comparable rates of external MTSET modification in depolarized channels, while at the negative potentials of −80 mV (356C, 359C, 365C) and −100 mV (362C) only modification of the three most N-terminal remained appreciable (whereas 365C modification became so slow as to be undetectable; Larsson et al., 1996). Figure 5A shows the results of a more detailed examination of the voltage dependence of 359C modification by external MTSET. It shows that hyperpolarization of A359C channels to voltages more negative than −80 mV leads to modification rates that are slower than the closed-channel rate that we reported previously. It also shows that the overall voltage dependence of the rate correlates with that of charge movement: the superimposed curve is a scaled mean Q-V obtained from nonconducting A359C channels. The observations that (1) external MTSET modification at −120mV was 80-fold slower than that seen for fully activated channels, and that (2) the residual rate might be attributed to the fractional gating charge remaining activated at −120 mV argue together that, in the resting state of Shaker channels, residue 359 is effectively buried.

We observed that hyperpolarization also progressively diminished the external modification rate of R362C channels: $k(-80\ mV) = 0.86 \pm 0.01\ mM^{-1}$, n = 3; $k(-100\ mV) = 0.51 \pm 0.02\ mM^{-1}\ s^{-1}$, n = 4; $k(-140\ mV) = 0.24 \pm 0.02\ mM^{-1}\ s^{-1}$, n = 3. Since attempts to obtain gating currents from nonconducting R362C channels were unsuccessful, it was not possible to determine where this voltage range lies with respect to the voltage dependence of gating-charge activation in these channels. This result leaves open the possibility that residue 362 is inaccessible in the resting channel state.

In contrast, hyperpolarization beyond −80 mV did not significantly affect the external MTSET modification rate of M356C channels [$k(-80mV) = 13 \pm 3\ mM^{-1}\ s^{-1}$, n = 6; $k(-120\ mV)\ 10.1 \pm 0.8\ mM^{-1}\ s^{-1}$, n = 3]. Thus, residue 356 appears to remain exposed to the external solution regardless of the channel gating state. Therefore, the external boundary of the buried tm segment of S4 in the resting channel state appears to lie between A359 and M356.

The active-state external boundary was determined

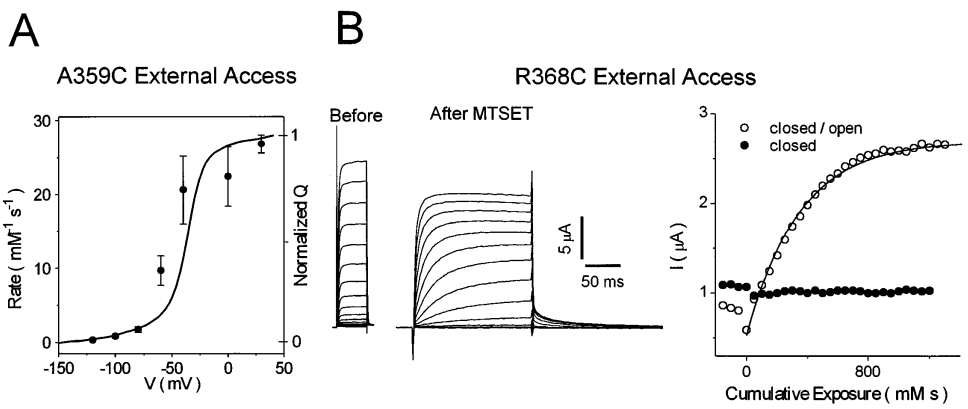

Figure 5. External MTSET Modification of 359C and Transmembrane Displacement of 368C

(A) Voltage dependence of the rate of modification of conducting A359C channels superimposed on the scaled Q-V (n = 4).

(B) R368C channel currents evoked by a series of steps ranging −40 to +140 mV in increments of 10 mV from the −80 mV hp, followed by V_{tail} = +10 mV before and after external MTSET exposure. Modified channels ("After MTSET") activate and deactivate more slowly, and depend more steeply on voltage than unmodified ones ("Before"). Graph shows superimposed time courses from a representative oocyte superfused with MTSET first while being clamped at −80 mV for 9.9 of every 10 s epoch ("closed" protocol), producing no effect, and immediately afterwards while depolarizing to +60 mV for 5 of every 10 s epoch ("closed/open" protocol), resulting in modification with monoexponential kinetics (superimposed curve, τ = 347 mM s). The implied rate is orders of magnitude slower than other externally modifiable S4 cysteines (Larsson et al., 1996; main text). Abscissa is [application time] × [MTSET concentration]. 0 marks onset of MTSET perfusion. Initial dip is likely partial blockade of channels by MTSET (5 mM), since a commensurate hop was always observed upon washout and the size scaled with ionic current amplitude. Points are the amplitude of ionic currents evoked by test pulses every 10 s to +60 mV measured 50 ms after the onset of each test step. Modification of 368C by *internal* MTSET at hyperpolarized potentials was shown in Larsson et al., 1996.

in our previous study to lie between residues R365 and R368: we observed no external MTSET modification of depolarized R368C channels even upon cumulative exposures 30-fold greater than those necessary to modify of R365C channels (Larsson et al., 1996). Figure 5B shows, however, that R368C channels are indeed modified by MTSET externally, but at an exceptionally low rate. Ionic currents recorded after modification exhibited slowed activation and tail kinetics and a steepened voltage dependence of channel opening like those of R368C channels modified by internal MTSET (Larsson et al., 1996). External modification was observed when channels were depolarized to +60 mV for 5 s of each 10 s epoch (Figure 5B, open circles), but not when channels were held at −80 mV 99% of the time (Figure 5B, closed circles). Depolarization to +120 mV did not accelerate modification beyond the rate observed for depolarization to +60 mV [k(+60 mV, 50%) = 0.0035 ± 0.00060 mM^{-1} s^{-1}, n = 3 versus k(+120 mV, 50%) = 0.0018 ± 8 × 10^{-6} mM^{-1} s^{-1}, n = 2]. We conclude that channel activation displaces 368C from a cytosolically accessible position (Larsson et al., 1996) to a position at or very near to the extracellular boundary.

These results adjust somewhat the tm boundaries of the extreme resting and activated states of S4, but preserve and add to the evidence that S4 movement underlies and can account for the gating-charge displacement observed in Shaker channels.

Figure 6 summarizes the MTSET modification-rate measurements for eight S4 substituted cysteines.

S4 Topology Is Consistent with Q_1 and Q_2 in R365C and wt

Figure 7A shows three topological states consistent with the accessibilities of eight S4 amino-acid positions in the resting and open states, as assayed previously (Larsson et al., 1996) and refined above, and consistent with the accessibilities of two positions (365 and 370) in an intermediate activated subunit state as deduced above. Assuming the tm electric field to be constant and confined entirely to the buried segment of S4, we calculated the amplitude of Q_1 and Q_2 implied by the two topologically resolved displacements illustrated in Figure 7A. For each displacement, we took the contribution of individual S4 basic residues to be equal to their fractional displacement through the transmembranous space, and took the total charge valence to be the sum of the individual residue contributions, δz (Figure 7B). This calculation fixes both the relative and absolute amplitudes of Q_1 and Q_2, and was performed for both the case where residue 365 is neutral (e.g., R365C), as well as for when it is positively charged (e.g., wt).

To test these predictions against the measured Q-Vs requires the postulation of a chemical-kinetic scheme of activation. A priori, either or both of the deduced topological changes in S4 might be proposed to arise from a concerted movement of the subunits. However, the "delay" or sigmoidicity in the rise of ionic currents implies a large number of transitional closed states (Zagotta et al., 1994a), and hence an independent enactment of two S4 displacements in all four subunits. A final concerted step is implied by multiple lines of evidence (Bezanilla et al., 1991; Schoppa et al., 1992; Tytgat and Hess, 1992; Zagotta et al., 1994a, 1994b; Schoppa and Sigworth, 1998; L. M. M. and E. Y. I., unpublished data; O. S. B. and E. Y. I., unpublished data) and is necessary to account for the disproportionate steepness of Q_2 (discussed above). Thus, the scheme of Figure 7C represents the simplest adaptation of our topological characterization of S4 to Shaker channel activation gating. Note

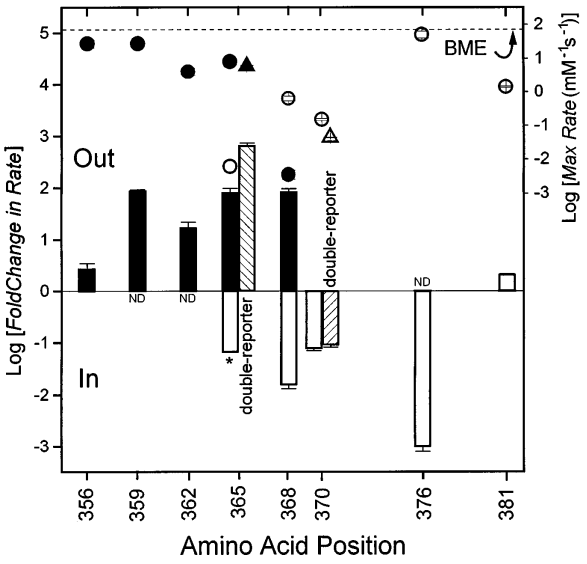

Figure 6. Summary of MTSET Rate Data for S4 Cysteines

Accessibility changes and maximal rates observed for MTSET modification of eight substituted S4 cysteines in this study and our previous study (Larsson et al., 1996), as well as those for internal 365C modification (*) observed by Holmgren and Yellen (personal communication). Bar height (plotted against the left-hand y-axis) equals the ratio of the rates observed at depolarized voltages over those at hyperpolarized voltages, and indicates state-dependent internal (open bars) and external (solid bars) accessibility. (Position 381 shows an upward-going open bar, because depolarization accelerated its internal modification.) Note that for external access of 365 and for internal access of 368, 370, and 376, the smaller of the two rates is a calculated upper limit (since in these cases modification was not observed at both hyperpolarized and depolarized potentials), estimated as described previously (Larsson et al., 1996). Data for the double-reporter channel (hatched bars) is shown beside 365 for external access and beside 370 for internal access. The maximum observed external (filled circles) and internal (open circles) modification rates are plotted against the right-hand y-axis. (Filled and open triangles refer, respectively, to external and internal modification of double-reporter channel.) BME = β-mercaptoethanol modification rate (Stauffer and Karlin, 1994), which indicates the expected rate for a maximally accessible cysteine. ND = not determined.

that the scheme is identical to that proposed by Sigworth (1994) and similar to that proposed by Zagotta et al. (1994b) in order to account for the detailed characteristics of Shaker gating and ionic currents.

All transitions including the final one were assumed to derive their voltage dependence from S4 movement. Under this assumption, the Q_2 topological change is the outcome of the second sequential subunit transition and the concerted step combined. The valence of the concerted step (z_c) was taken to be 1.8, consistent with the measurements of both Schoppa and Sigworth (1998) and ourselves (O. S. B. and E. Y. I., unpublished data) from ionic current and VCF recordings, respectively. The valence of the second sequential subunit transition was calculated to be the total predicted Q_2 valence minus $z_c/4$ (the per-subunit valence of the concerted step). The Q_1 topological change was interpreted to reflect the first sequential subunit transition, the valence of which was taken to be just that predicted for Q_1.

The three charge valences thus determined were tested against the measured Q-Vs employing the scheme of Figure 7C and allowing the voltage-midpoint parameters V_1, V_2, and V_C (Figure 7C legend) to vary. The excellent fit to the data described by the solid lines in Figure 1A demonstrates that the topological changes characterized (Figure 7A) are consistent with the voltage-dependence of charge movement of both R365C channels ("R365C"), as well as the high-resolution wild-type Q-V data of Bezanilla and coworkers ("wt"; data from Bezanilla et al., 1994).

Discussion

Topological Boundaries for Three S4 States in K^+ Channel Activation

The state-dependent accessibilities of 365C and 370C, as well as the pattern exhibited by six other singly substituted S4 cysteines, enable a description of the tm topology of S4 in three states of activation: two extreme states of S4 displacement—which were deduced previously (Larsson et al., 1996) and refined in this study—and an intermediate state of displacement in-between these two. The size of the two partial displacements is consistent with the observation that R365 neutralization divides charge movement into two like-sized components, together with studies suggesting that S4 carries most or all of the gating charge.

The cartoon of Figure 7A is one possible representation of the results of this and our previous study (Larsson et al., 1996), assuming a fixed α-helical spacing between S4 residues. Seven residues (359–365) are shown spanning the distance between the intracellular and extracellular solutions in deactivated channels (our experiments indicate the number to be between seven and nine), leaving two basic residues fully or partially buried (R362 and R365). The cartoon represents this buried length as 35% of the thickness of the bilayer hydrocarbon core (double-headed arrow, ~30 Å), or that expected for seven residues of α helix (Stryer, 1988). Thinning of the protein therefore must occur in the vicinity of S4. A relatively precipitous thinning around the external end of S4 might explain the gating state–dependent fluorescence of 365C-,359C-, and 356C-coupled fluors (Mannuzzu et al., 1996; Cha and Bezanilla, 1997). When channels activate, S4 moves outward as a unit in two sequential steps. The first correlates with Q_1 and buries F370 in the tm region. The second correlates with Q_2, exposes R365 to the extracellular solution, and leaves what is depicted as a total of ten residues buried (368–377; our experiments show this number to be between nine and twelve). Boundaries of the intermediate-state tm segment are not well constrained by experiment. The span is depicted as seven residues (365–371), the same number as in the resting state. Basic residues buried in the open state are shown proximal to acidic residues in S2 and S3 (circled minus symbols) as implied by the findings of Papazian and coworkers (Papazian et al., 1995; Tiwari-Woodruff et al., 1997).

Several aspects of the extreme resting and activated states represent refinements of our earlier conclusions. These include the inaccessibility of positions 359 and 362 in the resting state, and the proximity of 365 and

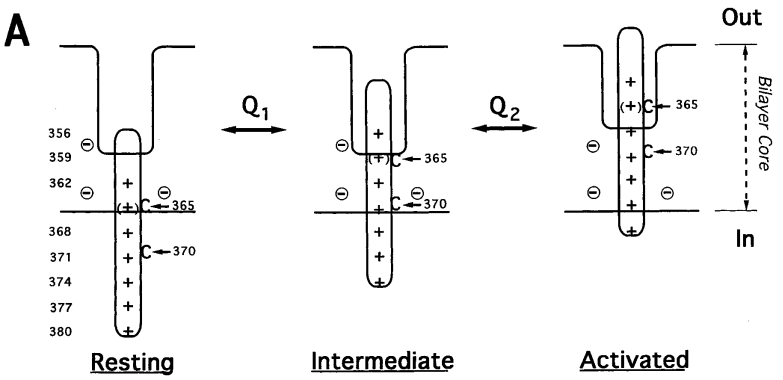

B

	$\delta z(Q_1)$	$\delta z(Q_2)$
362	0.5	0
365	0.86 *(0)*	0.07 *(0)*
368	0.5	0.45
371	0.07	0.58
374	0	0.35
377	0	0.05
380	0	0
Total	1.93 *(1.07)*	1.50 *(1.43)*

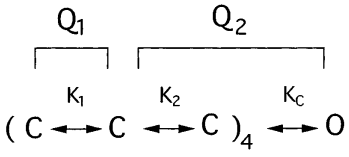

Figure 7. Two-Step Transmembrane Movement of the Shaker S4

(A) Region of protein around the S4 of a single subunit of the Shaker channel in the conformations associated with the deactivated, intermediate, and activated (open) states. When channels activate, S4 moves outward as a unit in two sequential steps. The first correlates with Q_1 and buries F370 in the transmembrane (tm) region. The second correlates with Q_2 and exposes R365 to the extracellular solution. The cartoon assumes a fixed α-helical spacing between S4 residues. Double-headed arrow is 30 Å, about the thickness of the hydrophobic core of the membrane bilayer (Stryer, 1988).

(B) The charge valences of Q_1 and Q_2 implied by the topologies in (A) were calculated as the sum of the incremental valences, δz, resulting from the displacements of individual S4 residues. Values in parentheses relate to R365-neutralized channels.

(C) A chemical-kinetic scheme that enables explanation of the Q-Vs of wt-activating and R365C channels (Figure 1A) on the basis of the topologies in (A). Two sequential displacements of S4 occur in each of the four subunits independently. A subsequent concerted step opens channels, effectively confers cooperativity to the second subunit transition and accounts for the disproportionate steepness of Q_2. In accordance with the gating-particle hypothesis of Hodgkin and Huxley (1952), the three equilibrium constants have expressions of the form

$$K_i = e^{z_i F(V - V_i)/RT}, (i = 1, 2, c)$$

where F, R, and T have their conventional meanings. The z_i of the gating scheme were fixed according to

$$z_1 = \Sigma\ \delta z(Q_1)$$

and

$$z_2 = [\Sigma\ \delta z(Q_2)] - \left(\frac{z_c}{4}\right),$$

with $z_c = 1.8$ determined independently from the valence of the final opening transition(s) (Schoppa and Sigworth, 1998; O. S. B. and E. Y. I., unpublished data). This formulation assumes that the shallow voltage-dependence of opening derives from a topologically unresolved S4 displacement occurring during Q_2. V_1, V_2, and V_c are the sole free parameters necessary to make equilibrium predictions from the topologically constrained scheme.

368 to solution interfaces in the resting and activated states, respectively.

"Interfacial" Positions

The external MTSET modification rate we observe for depolarized R368C channels is three to four orders of magnitude slower than that which we observe for depolarized M356C, A359C, R362C, and R365C channels (Figure 6). Holmgren and Yellen (personal communication) report a similar rate for hyperpolarized R365C channels under modification by *internal* MTSET (Figure 6). Clamping to −150 mV, the approximate half-activation point for Q_1, they observed internal 365C modification at a rate of ~0.005 $mM^{-1}\ s^{-1}$, while we observed a rate of 0.0035 $mM^{-1}\ s^{-1}$ for 368C externally, depolarizing 50% of the time. (Note that, using patches excised from mammalian cells, they achieved greater cumulative MTSET exposures at hyperpolarized voltages than ourselves, and so were able to observe 365C modify internally even though we were not.)

The exceptionally low modification rates of 365C in resting channels and of 368C in open channels admit at least two possible interpretations. One is that they reflect an exceptionally low cysteine accessibility state of the protein. Another is that modification accumulates slowly due to transitory sojourns—as might accompany protein "breathing" (Creighton, 1993)—from an inaccessible state of the channel to a short-lived accessible one. Both interpretations suggest a location for these residues near to the boundaries of the tm S4 segment, which is what has been depicted in Figure 7A. Neither interpretation appears to conflict with the observation of proton access to these positions (Starace et al., 1998), or with charge quantitation studies (Aggarwal and MacKinnon, 1996; Seoh et al., 1996) suggesting that R368 accounts for 1 e_o per subunit, and therefore traverses the entire tm electric field.

Na^+ and K^+ Channel S4s

The refined boundaries described above also increase the congruence between the deduced topologies of the domain-IV S4 of the Na channel hSkMI and that of the S4 of Shaker K channels. If S4 basic residues are numbered by the order of their appearance in the primary sequence, then studies of both channels (Larsson et al., 1996; Yang et al., 1996, 1997; this paper) predict R1 as

the sole inaccessible basic residue in the resting state, R2 and R3 as traversing the entire distance from inside to outside (just barely, in Shaker channels), and R4 and R5/K5 as inaccessible in the open state. Both studies predict internal R6 accessibility in resting channels, and neither makes explicit predictions about R6 accessibility in open channels. (Note that while Figure 7A depicts R6 as inaccessible in the open state, placement of the internal tm boundary anywhere between 376 and 380 would be consistent with our results; Yang and coworkers [1997] report that R6C depolarized access is currently under investigation.)

Channel Gating Mechanism

The results of this study have a number of implications regarding the mechanism of channel gating. One is that an auxiliary gating particle domain does not appear necessary to account for the existence of two components in the gating current records from Shaker channels. Another is that biophysical models of ionic and gating currents, which have hypothesized distinct types of voltage-dependent transitions and more than four closed channel states, appear to be justified on structural as well as on electrophysiological/theoretical grounds.

Our topological findings may also offer further insights into the mechanism of S4 translocation. The Figure 7A cartoon is consistent with the helical-screw mechanism of S4 displacement (Catterall, 1988; Guy and Conti, 1990). Assuming such a mechanism implies that an equivalent 120 degree rotation and 6 a.a. displacement of S4 would underlie both Q_1 and Q_2, and would cause the exchange of S4 charges with their second nearest neighbors in salt bridges with fixed counter charges in, for example, S2 and S3.

S4 Movement, Mutagenesis, and Voltage-Sensing Diversity

One conundrum in structure–function studies of voltage-gated channels has been that even charge-conserving S4 amino acid substitutions can dramatically affect the voltage sensitivity of channel opening (Sigworth, 1994). We have shown that a point mutation can change the relative stabilities of three states of S4 displacement, causing an intermediate state to predominate at the cell resting potential (V_{rest}). Under such a circumstance, a significant component of the gating charge is already activated at V_{rest} and thus does not contribute to the steepness with which channel opening depends on voltage (except to the limiting slope on a log plot). Therefore, our results establish a mechanism by which an amino acid substitution can affect the voltage sensitivity of channel opening without actually altering S4 "valence."

More broadly, the results suggest why, among members of the S4-superfamily of voltage-gated channels, S4 valence is a poor predictor of voltage sensitivity. The similar topological extremes observed for the Shaker potassium channel S4 and the domain-IV S4 of hSkMI sodium channels suggest that *high* voltage sensitivity is achieved by a common mechanism, even in evolutionarily divergent channels (Shaker and skeletal-muscle sodium channels have a similar total gating charge; 12.3–13.6 e_o and 12 e_o, respectively; Schoppa et al., 1992; Hirschberg et al., 1995; Aggarwal and MacKinnon, 1996; Seoh et al., 1996). But the "gating phenotype" of R365C channels suggests that less voltage-sensitive channels may have arisen from an abridgment of S4 motion.

We suggest that the possibility of abridged S4 motion be considered in interpreting the reduction of total gating charge resulting from mutagenesis (Aggarwal and MacKinnon, 1996; Seoh et al., 1996; Starace et al., 1998). In R365C channels, Q_1 does not escape detection, because it deactivates within the range of voltages that can be obtained (for short durations) by voltage clamp. But this need not always be so. For example, Starace and coworkers have recently reported (1998) that increasing pH reduces the gating charge of R365H Shaker channels from 12.5 to 3.5 e_o, i.e., considerably more than can be accounted by the neutralization of one charge per subunit. Abridged S4 motion could also result in a misinterpretation of the role of charged residues. In the case of the exceptionally large decrement in gating charge reported for the E293Q substitution (Seoh et al., 1996), for example, a relative destabilization of the most retracted state of S4 is a plausible explanation, especially in light of the native residue's apparent role in a buried salt bridge with S4 (Papazian et al., 1995; Tiwari-Woodruff et al., 1997).

Experimental Procedures

Channels

All experiments were performed on Shaker channels made incapable of fast-inactivation by the Δ(6–46) deletion (Hoshi et al., 1990). Gating currents were recorded from channels with the W434F mutation, which prevents conduction (Perozo et al., 1993). Shaker H4 (Kamb et al., 1987) Δ(6–46) and Δ(6–46)/W434F plasmid DNAs were gifts of Ligia Toro. We use "wild type–activating" throughout the text to refer to 434F and 434W channels interchangeably, since the W434F substitution has been shown not to alter gating-charge movement (Perozo et al., 1993). Cysteines were substituted at specific S4 positions by Kunkel mutagenesis. To prevent fluorescent labeling outside S4, the native cysteines 245 and 462 were substituted with valine and alanine, respectively. All gating currents were recorded in this genetic background. cRNA-encoding conducting channels was transcribed in vitro and injected into *Xenopus laevis* oocytes as described previously (Larsson et al., 1996). cRNA for gating currents was transcribed using the T7 mMessage mMachine kit protocol (Ambion, Austin Texas) and injected at approximately 1 g/l concentration.

Electrophysiology and Voltage Clamp Fluorometry

Conducting channels were recorded by patch- and by two-electrode voltage clamp as described previously (Larsson et al., 1996). Gating current recording was performed using a Dagan CA-1 amplifier (Dagan Corporation, Minneapolis, MN) in two-electrode voltage clamp mode, external solution 110 mM $NaCH_3SO_3$, 2 mM $Ca(CH_3SO_3)_2$, 10 mM HEPES (pH 7.5); bridges 1 M $NaCH_3SO_3$, 10 mM HEPES (pH 7.5). Background capacity of the native membrane was neutralized by compensating transients evoked by +20 mV depolarizations from an hp of +60 mV. Voltage clamp fluorometry (VCF) was performed as previously described (Mannuzzu et al., 1996).

Accessibility Probing

General

The internal and external accessibility of S4-substituted cysteines to the membrane-impermeant thiol reagent, MTSET (Toronto Research Chemicals), was assayed functionally in two electrode voltage-clamped and patch-clamped oocytes, as described earlier (Larsson

et al., 1996). The second-order rate constant of modification for any given set of conditions was calculated based on the average time constant, τ (units [concentration of MTSET] $\times$ [perfusion duration]), of a monoexponential fit to the time course of modification. For those experiments in which channels were clamped to a single voltage, except for brief test pulses, or for patch experiments in which MTSET was applied periodically during only a particular epoch of the voltage protocol, the rate of modification, k, was calculated simply as τ^{-1}. In other cases, MTSET was perfused continuously while oocytes were clamped alternately to the hp and to a distinct assay potential. For these assays the rate was calculated according to

$$k = A^{-1}[\tau^{-1} - (1 - A)k_{hp}]$$

where A is the fraction of the time the oocyte was held depolarized (usually 0.5), and k_{hp} is the rate of modification at the hp. k_{hp} was determined from experiments in which the hp was the exclusive or predominant voltage (as described for the simple rate determination). Contamination of rate measurements due to the accumulation of modification during the brief steps to the voltage used to monitor current was in all instances calculated to be less than the experimental scatter in the measurements.

A Note Regarding Nomenclature. Since it is possible to measure a modification rate at voltages at which channels (or rather subunits) are equilibrating between a number of voltage-dependent conformations, we use "modification rate" and "modifiability" in reference to a *population*, and reserve "accessibility" and "rate of accessibility" for characteristizating a specific conformational *state*.

Specific Assays

In general, the modification protocols employed in this study are the same as those described in the earlier study (Larsson et al., 1996). Particulars have been noted in the figure legends. Some specific considerations apply to the R365C/F370C or "double-reporter" channels. R365C channels modified by MTSET undergo a shift of approximately −80 mV in their voltage dependence of opening, so that modification by MTSET can be monitored as an increase in conductance at negative potentials (Larsson et al., 1996). R365C/F370C channels modified by external MTSET also undergo a shift of approximately −80 mV in their voltage dependence of opening, but the modified channels undergo rapid C-type (Hoshi et al., 1991) inactivation at a hp of −80 mV (data not shown). External MTSET modification of R365C/F370C channels, therefore, was monitored as a decrease in the test-pulse current. The assay voltage, +80 mV (at the top of the G/V), was applied in steps that were separated by intervals of sufficient duration to reach a steady-state with respect to the C-type inactivation of modified channels. To be able to exclude trials in which run-down contaminated the time course, the membrane was hyperpolarized following modification to induce recovery from C-type inactivation and thus to verify that currents returned to their initial levels. In cases of unusually robust oocytes a −140 mV hp could be used, at which voltage no inactivation accumulated; and modification by MTSET was monitored, as for R365C channels (Larsson et al., 1996), by the increase in conductance at negative potentials. The rates of MTSET modification determined by the two methods were very similar.

F370C channels modified by MTSET cease to conduct in response to test depolarizations even as large as 160 mV, even when preceded by extreme hyperpolarization. Thus, the effects of MTSET conjugation at positions 365 and 370 were distinguishable. This ability was used to advantage in interpreting modification of R365C/F370C double mutant channels.

Charge Reconstitution Assay

MTSEA (Toronto Research Chemicals) was chosen over MTSET because modification by the latter was observed in initial trials to slow channel gating currents so greatly that we could not accurately measure them. The Q-V of "charge-reconstituted" channels was determined from gating currents measured from R365C and R365C/F370C channels immediately following 1–20 mM s cumulative MTSEA exposure (10 μM) during stimulus trains of 5 s long steps to +50 mV applied once every 10 s (hp −80 mV), during which test pulse-evoked gating currents were observed to increase and to saturate. After washout, gating currents from the modified channels diminished with time, making difficult a quantitation of the absolute charge increase caused by modification. Since the G-V of both channels is shifted to very negative potentials by MTSEA modification (unpublished observations), the apparent decrease in gating current amplitude may be associated with slow inactivation.

Accessibility Reconstitution Assay

The internal accessibility of 370C in R365C-SEA/F370C channels was assayed by external preexposure of non-voltage-clamped oocytes to 2 mM s MTSEA (three times the time-constant of modification under voltage clamp as described above) during a 30 s incubation in a depolarizing solution (89 mM KCl, 0.8 mM $MgCl_2$, 0.4 mM $CaCl_2$, 10 mM HEPES [pH 7.5]), followed by excision of inside-out patches and internal accessibility assay as described above.

Analysis and Modeling

Basic analysis of recordings was performed using pClamp6 (Axon Instruments, Foster City, CA). Secondary analysis was performed using Origin (Microcal Software, Inc., Northampton, MA) for curve fitting of simple functions and using Madonna (YouSee Software, Berkeley, CA) for fitting to chemical-kinetic models. Values in the text are expressed as mean ± SEM, except where otherwise noted.

Theoretical Q-V Curves

All Q-V data was fit to the sum of two Boltzmann functions (Figure 1A legend). Q-V data from R365C channels and from wild-type activating channels (Figure 1A) was also fit to the predicted Q-V for the model of Figure 7C:

$$Q = Ne_o\zeta^{-1}\begin{bmatrix} 4z_1K_1 + 6(2z_1K_1^2) + 4(3z_1K_1^3) + (4z_1K_1^4) + \\ 4(z_1 + z_2)K_1K_2 + 12(2z_1 + z_2)K_1^2K_2 + \\ 6(2z_1 + 2z_2)K_1^2K_2^2 + 12(3z_1 + z_2)K_1^3K_2 + \\ 12(3z_1 + 2z_2)K_1^3K_2^2 + 4(3z_1 + 3z_2)K_1^3K_2^3 + \\ 4(4z_1 + z_2)K_1^4K_2 + 6(4z_1 + 2z_2)K_1^4K_2^2 + \\ 4(4z_1 + 3z_2)K_1^4K_2^3 + (4z_1\ 4z_2)K_1^4K_2^4 + \\ (4z_1 + 4z_2 + z_c)K_1^4K_2^4K_c \end{bmatrix}$$

where

$$\zeta = (1 + K_1 + K_1K_2)^4 + K_1^4K_2^4K_c$$

is the partition function. Sixteen channel states are implied by the scheme of 7C under the assumption of four identical subunits, and each is reflected by a term in ζ, upon expansion of the term in parentheses. The term in square brackets in the Q-V is simply each term in ζ weighted by the appropriate charge valence. e_o is the fundamental electronic charge and N equals the number of channels. The normalized Q-V relation results by dividing the above expression by

$$Q_{max} = Ne_o(4z_1 + 4z_2 + z_c)$$

However, due to the extreme voltages involved, it was not usually possible to obtain R365C channel Q-Vs that completely saturated at the negative voltage extreme. Therefore, they could not be precisely normalized, and the amplitude was left as a free parameter even in the fitting of the roughly normalized Q-Vs. (For the model Q-V equation, this was done by using the unnormalized expression and allowing N to vary, for the double-Boltzmann by *not* using the constraint $Q_1 + Q_2 = 1$.) The fitted amplitudes of the double-Boltzmann and the model were not usually equal. As is visible in Figure 1A, the double-Boltzmann fit predicts a larger amplitude and lower valence (z_1) for Q_1 than does the model.

Acknowledgments

We thank Rena Yamamoto for assistance with experiments and analysis, Lloyd Llewelyn for technical assistance, and the other members of the Isacoff Lab for discussions and helpful suggestions. Funded by N. I. H., grant #R01NS35549, AHA, California Affiliate Grant #94-216; E. Y. I. is a fellow of the Klingenstein and of the McKnight Foundation, H. P. L. is a Wenner-Gren Fellow, and L. M. M. is an AHA postdoctoral fellow, California Affiliate Grant #95-41.

Received January 23, 1998; revised April 24, 1998.

References

Aggarwal, S.K., and MacKinnon, R. (1996). Contribution of the S4 segment to gating charge in the Shaker K^+ channel. Neuron *16*, 1169–1177.

Akabas, M.H., Stauffer, D.A., Xu, M., and Karlin, A. (1992). Acetylcholine receptor channel structure probed in cysteine-substitution mutants. Science *258*, 307–310.

Bezanilla, F., Perozo, E., Papazian, D.M., and Stefani, E. (1991). Molecular basis of gating charge immobilization in Shaker potassium channels. Science *254*, 679–683.

Bezanilla, F., Perozo, E., and Stefani, E. (1994). Gating of Shaker K^+ channels: II. The components of gating currents and a model of channel activation. Biophys. J. *66*, 1011–1021.

Catterall, W.A. (1988). Structure and function of voltage-sensitive ion channels. Science *242*, 50–61.

Cha, A., and Bezanilla, F. (1997). Characterizing voltage-dependent conformational changes in the Shaker K^+ channel with fluorescence. Neuron *19*, 1127–1140.

Creighton, T.E. (1993) Proteins: Structures and Molecular Properties (New York: W. H. Freeman and Co.).

Greenblatt, R.E., Blatt, Y., and Montal, M. (1985). The structure of the voltage-sensitive sodium channel. Inferences derived from computer-aided analysis of the *Electrophorus electicus* channel primary structure. FEBS Lett. *193*, 125–134.

Guy, H.R., and Conti, F. (1990). Pursuing the structure and function of voltage-gated channels. Trends Neurosci. *13*, 201–206.

Guy, H.R., and Seetharamulu, P. (1986). Molecular model of the action potential sodium channel. Proc. Natl. Acad. Sci. USA *83*, 508–512.

Hirschberg, B., Rovner, M., Lieberman, M., and Patlak, J. (1995). Transfer of twelve charges is needed to open skeletal muscle Na^+ channels. J. Gen. Physiol. *106*, 1053–1068.

Hodgkin, A.L., and Huxely, A.F. (1952). A quantitative description of membrane current and its application to conduction and excitation in nerve. J. Physiol. (Lond.) *117*, 500–544.

Hoshi, T., Zagotta, W.N., and Aldrich, R.W. (1990). Biophysical and molecular mechanisms of Shaker potassium channel inactivation. Science *250*, 533–538.

Hoshi, T., Zagotta, W.N., and Aldrich, R.W. (1991). Two types of inactivation in Shaker K^+ channels: effects of alterations in the carboxy-terminal region. Neuron *7*, 547–556.

Kamb, A., Iverson, L.E., and Tanouye, M.A. (1987). Molecular characterization of Shaker, a Drosophila gene that encodes a potassium channel. Cell *50*, 405–413.

Larsson, H.P., Baker, O.S., Dhillon, D.S., and Isacoff, E.Y. (1996). Transmembrane movement of the Shaker K^+ channel S4. Neuron *16*, 387–397.

Mannuzzu, L.M., Moronne, M.M., and Isacoff, E.Y. (1996). Direct physical measure of conformational rearrangement underlying potassium channel gating. Science *271*, 213–216.

McCormack, K., Joiner, W.J., and Heinemann, S.H. (1994). A characterization of the activating structural rearrangements in voltage-dependent Shaker K^+ channels Neuron *12*, 301–315. Erratum: (1994). Neuron *12*, 706.

Noda, M., Shimizu, S., Tanabe, T., Takai, T., Kayano, T., Ikeda, T., Takahashi, H., Nakayama, H., Kanaoka, Y., and Minamino, N., et al. (1984). Primary structure of *Electrophorus electricus* sodium channel deduced from cDNA sequence. Nature *312*, 121–127.

Papazian, D.M., Shao, X.M., Seoh, S.A., Mock, A.F., Huang, Y., and Wainstock, D.H. (1995). Electrostatic interactions of S4 voltage sensor in Shaker K^+ channel. Neuron *6*, 1293–1301.

Perozo, E., MacKinnon, R., Bezanilla, F., and Stefani, E. (1993). Gating currents from a nonconducting mutant reveal open-closed conformations in Shaker K^+ channels. Neuron *11*, 353–358.

Schoppa, N.E., McCormack, K., Tanouye, M.A., and Sigworth, F.J. (1992). The size of gating charge in wild-type and mutant Shaker potassium channels. Science *255*, 1712–1715.

Schoppa, N.E., and Sigworth, F.J. (1998). Activation of Shaker potassium channels. III. An activation gating model for wild-type and V2 mutant channels. J. Gen. Physiol. *111*, 313–342.

Seoh, S.A., Sigg, D., Papazian, D.M., and Bezanilla, F. (1996). Voltage-sensing residues in the S2 and S4 segments of the Shaker K^+ channel. Neuron *16*, 1159–1167.

Sigg, D., Stefani, E., and Bezanilla, F. (1994). Gating current noise produced by elementary transitions in Shaker potassium channels. Science *264*, 578–582.

Sigworth, F.J. (1994). Voltage gating of ion channels. Quart. Rev. Biophys. *27*, 1–40.

Stauffer, D.A., and Karlin, A. (1994). Electrostatic potential of the acetylcholine binding sites in the nicotinic receptor probed by reactions of binding-site cysteines with charged methanethiosulfonates. Biochemistry *33*, 6840.

Starace, D.M., Stefani, E., and Bezanilla, F. (1998). Voltage-dependent proton transport by the voltage sensor of the Shaker K^+ channel. Neuron *19*, 1319–1327.

Stefani, E., Toro, L., Perozo, E., and Bezanilla, F. (1994). Gating of Shaker K^+ channels: I. Ionic and gating currents. Biophys. J. *66*, 996–1010.

Stryer, L. (1988). Biochemistry (New York: W. H. Freeman and Co.).

Stuhmer, W., Conti, F., Stocker, M., Pongs, O., and Heinemann, S.H. (1991). Gating currents of inactivating and non-inactivating potassium channels expressed in Xenopus oocytes. Pflugers Arch. *418*, 423–429.

Tiwari-Woodruff, S.K., Schulteis, C.T., Mock, A.F., and Papazian, D.M. (1997) Electrostatic interactions between transmembrane segments mediate folding of Shaker K^+ channel subunits. Biophys. J. *72*, 1489–1500.

Tytgat, J., and Hess, P. (1992). Evidence for cooperative interactions in potassium channel gating. Nature *359*, 420–423.

Yang, N., George, A.L., Jr., and Horn, R. (1996). Molecular basis of charge movement in voltage-gated sodium channels. Neuron *16*, 113–122.

Yang, N., and Horn, R. (1995). Evidence for voltage-dependent S4 movement in sodium channels. Neuron *15*, 213–218.

Yang, N., George, A.L., Jr., and Horn, R. (1997). Probing the outer vestibule of a sodium channel voltage sensor. Biophys. J. *73*, 2260–2268.

Yusaf, S.P., Wray, D., and Sivaprasadarao, A. (1996). Measurement of the movement of the S4 segment during the activation of a voltage-gated potassium channel. Pflugers Arch. *433*, 91–97.

Zagotta, W.N., Hoshi, T., Dittman, J., and Aldrich, R.W. (1994a). Shaker potassium channel gating. II: Transitions in the activation pathway. J. Gen. Physiol. *103*, 279–319.

Zagotta, W.N., Hoshi, T., and Aldrich, R.W. (1994b). Shaker potassium channel gating. III: Evaluation of kinetic models for activation. J. Gen. Physiol. *103*, 321–362.